JACS
JOURNAL OF THE AMERICAN CHEMICAL SOCIETY
Communication
pubs.acs.org/JACS

Supramolecular Precursors for the Synthesis of Anisotropic Cu_2S Nanocrystals

Whitney Bryks, Melissa Wette, Nathan Velez, Su-Wen Hsu, and Andrea R. Tao*

Department of NanoEngineering, University of California, San Diego, 9500 Gilman Drive MC 0448, La Jolla, California 92039-0448, United States

Supporting Information

ABSTRACT: Copper alkanethiolates are organometallic precursors that have been used to form Cu_2S nanodisks upon thermal decomposition. Here, we demonstrate that molecular assembly of Cu alkanethiolates into an ordered liquid crystalline mesophase plays an essential role in templating the disk morphology of the solid-state product. To examine this templating effect, we synthesize Cu alkanethiolate precursors with alkane tails of varying chain length and sterics. We demonstrate that short chain precursors produce two-dimensional (2D) nanosheets of Cu_2S, while longer-chained variants produce Cu_2S nanodisks exclusively. This work provides new insights into the use of liquid crystalline phases as templates for nanocrystal synthesis and as a potential route for achieving highly anisotropic inorganic nanostructures.

Copper sulfide nanomaterials are p-type semiconductors that are being explored for applications in photovoltaics,[1] electrochemical sensors,[2] and battery electrodes.[3] More recently, colloidal chalcocite (Cu_2S) nanocrystals have gained interest as a plasmonic material that is capable of supporting the excitation of localized surface plasmon resonances.[4−7] Cu_2S nanocrystals exhibit tunable optical resonances in the near- to mid-infrared range[7] and have the potential to enable strong near-field localization (i.e., light focusing) at these frequencies. Because anisotropic nanostructures are known to support the strongest field localizations,[8,9] fabricating highly anisotropic Cu_2S nanostructures will be a major challenge for plasmonic applications. Toward this end, we and others have investigated the optical resonances of colloidal Cu_2S nanocrystals such as shells,[10] rods,[11] wires,[12] and disks.[6] It would be highly advantageous to be able to synthesize colloidal Cu_2S nanocrystals with these anisotropic morphologies in a controlled, rational manner.

One common method for synthesizing colloidal Cu_2S nanocrystals is via thermolysis of Cu thiolates, which behave as a single-source molecular precursor. This method of solventless thermolysis was first reported by Sigman et al.,[13] who synthesized Cu_2S nanodisks from the thermal treatment of Cu dodecanethiolate ($CuSC_{12}H_{25}$). In these studies, nanodisk formation was attributed to faster deposition at the high surface energy facets that comprise the disk edges, facilitating radial growth. However, nanodisk size and aspect ratio were limited to a narrow range, which is not accounted for by this growth mechanism. In a later work, Chen et al. also carried out solventless thermolysis at 200−220 °C with $CuSC_{12}H_{25}$.[14] Their precursor was shown to have a lamellar structure at room temperature, and the formation of nanodisks was attributed to the aggregation of small Cu_2S nucleates constrained within this lamellar structure. The decomposition of $CuSC_{12}H_{25}$ was also investigated by Wang et al. using the hot injection method, where copper sulfide is obtained using a solvent-based synthesis at temperatures between 160 and 220 °C.[15] In their study, lamellar $CuSC_{12}H_{25}$ was identified as the precursor to copper sulfide formation. However, both of the above studies did not account for melting of the lamellar $CuSC_{12}H_{25}$ structure (∼140 °C),[16] which occurs well below the thermolysis temperatures used in their experiments.

Herein we report an alternative mechanism for the synthesis of anisotropic Cu_2S nanodisks and nanosheets via solventless thermolysis, where shape control is enabled by the formation of a liquid crystal-like molecular template. Metal alkanethiolates are known to form mesogenic phases due to hydrophobic interactions between neighboring alkane chains and strong metal−sulfur coordination.[17] We investigate the thermolysis of various Cu thiolates that adopt lamellar, micellar, and isotropic (disordered) phases at the thermolysis reaction temperature and examine how these phases template the nucleation and growth of solid-state Cu_2S nanocrystals. We observe that Cu_2S nanodisks form only from Cu alkanethiolate precursors that adopt an inverse columnar mesophase, while flat 2D Cu_2S nanosheets form from precursors that adopt a lamellar phase at the thermolysis temperature. We also observe that isotropic phases give rise to nanocrystals that exhibit little-to-no shape control. These results provide new insights into the shape control mechanism for Cu_2S nanodisks and provide a rational route for producing highly anisotropic Cu_2S nanostructures.

Cu thiolate precursors are prepared by precipitating an aqueous solution of $Cu(NO_3)_2$ with the desired alkylthiol. A detailed procedure may be found in the Supporting Information. Cu alkanethiolates were synthesized with alkyl backbone chain lengths of n = 4, 8, 12, or 16 carbons. Figure S1 shows the XRD spectra (Rigaku RU200B) of these precursors. The periodically spaced low-angle peaks from $2\theta = 5°−19°$ are attributed to multiple reflections (kd, where k is an index and d is spacing) characteristic of a lamellar solid (Figure 1a, left). These peaks are fully indexed in Figure S1 and show an increase in d-spacing from 1.59 to 4.55 nm as the alkyl chain increases from 4 to 16 methylene units. Our thermogravimetric

Received: January 27, 2014
Published: April 8, 2014

   dx.doi.org/10.1021/ja500786p | J. Am. Chem. Soc. 2014, 136, 6175−6178

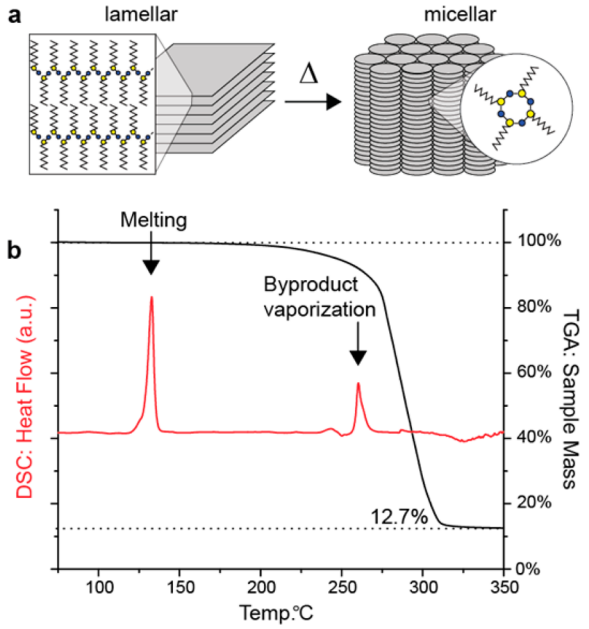

Figure 1. Thermal Properties. Schematic diagrams of the lamellar to mesophase transformation upon melting (a), and overlaid TGA and DSC curves for $CuSC_{12}H_{25}$ (b).

analysis (PerkinElmer TGA 7) measurements for $CuSC_{12}H_{25}$ show the loss of alkyl sulfides and disulfides to yield the solid-state Cu_2S product, which is obtained as a black powder (Figure 1b). Mass retention is ~4% lower than expected, likely indicating a nonstoichiometric yield of Cu_2S. Based on our thermal characterization, we carried out thermolysis of Cu alkanethiolates at or near 200 °C.

We visually observed melting of the supramolecular $CuSC_{12}H_{25}$, which was corroborated by a strong endothermic peak measured by differential scanning calorimetry (PerkinElmer PYRIS Diamond) at 132 °C (Figure 1b). Previously, Sigman and Chen attributed this endothermic peak to C−S bond thermolysis.[13,14] However, TGA shows that thermolysis occurs at much higher temperatures. Thus, we attribute the peak to a melting phase transition. Previous reports for Cu alkanethiolates indicate that these mesogens undergo a lamellar-to-micellar phase transition at approximately 140 °C.[16,18] These micellar columns are composed of stacked discotic micelles, where alkyl chains trail radially from the micelle edges (Figure 1a, right).[16] Cu alkanethiolates likely adopt this columnar mesophase during thermolysis, which is carried out well above 140 °C. As confirmation, we isolated one-dimensional "strings" or columns of mesogenic $CuSC_{12}H_{25}$ upon thermal annealing above the melting transition (Figure S2).

For the short-chained Cu alkanethiolate ($CuSC_4H_9$), no melting transition is observed prior to thermolysis at 200 °C. However, we observe that the precursor changes color from dark yellow to orange before gradual blackening of the powder. This color change is attributed to a transition from the crystalline lamellar phase to a smectic-like lamellar phase, which is known to occur for short-chain Ag alkanethiolates (n = 4–10).[19] This color change is accompanied by an endothermic peak on the DSC curve at around 160 °C (Figure S3). Thus, we expect the thermolysis product of supramolecular $CuSC_4H_9$ to be templated by a lamellar structure. The resulting thermolysis product showed significant signs of oxidation, likely due to poor surface passivation of the resulting Cu_2S nanocrystals by the short butyl chains. To address this issue, we carried out $CuSC_4H_9$ decomposition under N_2 flow for 24 h at 200 °C. These significantly longer reaction times are necessary for oxygen-free conditions, which have been demonstrated to decrease the thermolysis reaction rate.[20]

To characterize all of the solid-state products obtained by thermolysis, we carried out transmission electron microscopy (TEM, FEI Tecnai G2 Sphera) on samples prepared by dispersing the Cu_2S product in ethanol and drop-casting the dispersion directly onto a carbon-coated support grid. Figure 2 shows TEM images of the resulting nanocrystals obtained by solventless thermolysis of the Cu alkanethiolates. For n = 8–16, disk-like particles were obtained. Nanodisks obtained from the thermolysis of $CuSC_8H_{17}$ display the greatest polydispersity, with an average diameter of 21.48 ± 15.95 nm and average thickness of 3.66 ± 0.87 nm. These disks were found among many smaller, mostly ovoid particles ranging from 2 to 12 nm in size. Nanodisks obtained from $CuSC_{12}H_{25}$ possess an average diameter of 25.76 ± 5.83 nm and an average thickness of 5.47 ± 0.68 nm. Nanodisks obtained from $CuSC_{16}H_{33}$ were 23.50 ± 5.25 nm in diameter and 7.80 ± 1.09 nm thick. FTIR spectra indicate that all disks are terminated with alkyl groups (Figure S4). This surface passivation renders the disk surface hydrophobic, causing them to preferentially assemble into face-to-face stacks.

Figure 2d shows XRD spectra obtained for the resulting Cu_2S nanodisks. The nanodisks are composed mainly of high-temperature β-chalcocite, with some Cu-deficient $Cu_{1.96}S$ present. Several peaks from 2θ = 31°–34° that are unidentifiable with chalcocite are also present. These peaks likely stem from the significant amount of Cu deficiencies that are symptomatic of solventless thermolysis carried out under ambient atmosphere (due to Cu oxidation).

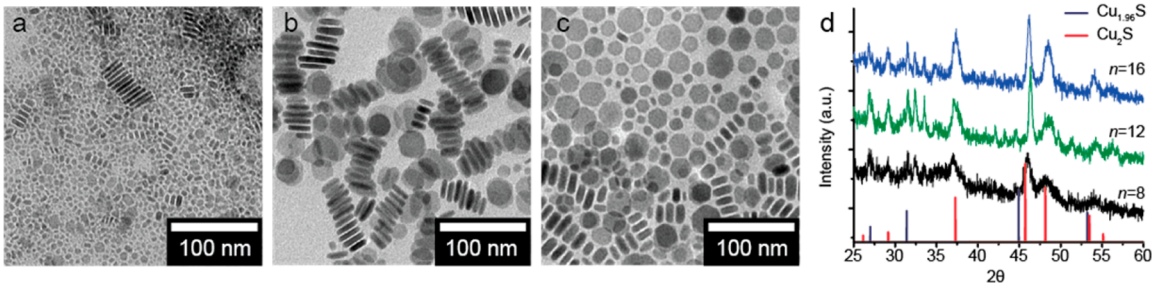

Figure 2. Cu_2S Nanodisks. TEM images of the products obtained from the solventless thermolysis of copper alkanethiolates: $CuSC_8H_{17}$ (a), $CuSC_{12}H_{25}$ (b), and $CuSC_{16}H_{33}$ (c), and the corresponding XRD patterns (d).

dx.doi.org/10.1021/ja500786p | J. Am. Chem. Soc. 2014, 136, 6175–6178

Nanocrystals obtained from the thermolysis of $CuSC_8H_{17}$ are notably heterogeneous in comparison to products from the longer-chained Cu alkanethiolates. Alkyl chain length is likely to affect the stability of the resulting columnar mesophase. We observe that shorter alkyl chains fail to induce the columnar mesophase transition; at least an 8-carbon chain is required to observe sample melting, and a 12-carbon chain is required to produce monodisperse nanodisks. It is likely that an 8-carbon chain is long enough to induce melting to form a columnar mesophase, but results in only partial phase ordering. This dependence of phase stability on chain length is similar to the observation made for self-assembled monolayers (SAMs), where 10-carbon chains have been shown as the minimum chain length required to produce a well-ordered, solidly packed SAM on Cu.[21]

Nanocrystals obtained from the thermolysis of supramolecular $CuSC_4H_9$ do not possess a disk-like shape and instead adopt a sheet structure (Figure 3a). The nanosheets vary in length from 50 nm platelets to ribbons over 1 μm long. Atomic force microscopy (AFM, Bruker Scanning Probe Microscope) measurements reveal that the nanosheets are 5.4 $\pm$ 1.7 nm thick and that this thickness is fairly consistent across a nanosheet (Figure 3b,c and Figure S5). This 2D morphology is consistent with thermolysis of the lamellar $CuSC_4H_9$ precursor, which we believe is responsible for templating these planar structures. XRD spectra indicate that the nanosheets are composed of the low temperature α-chalcocite phase (Figure 3d).

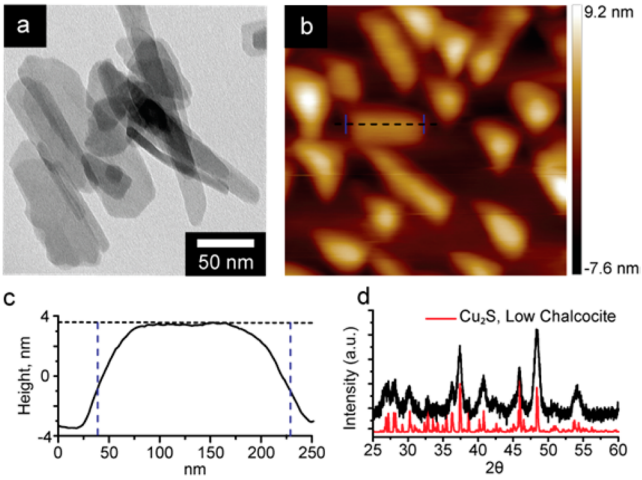

Figure 3. Cu_2S Nanosheets. TEM image of the Cu_2S nanosheets from thermally decomposed $CuSC_4H_9$ (a), AFM topology image of nanosheets (b), AFM height profile of a nanosheet displaying a thickness of 7.5 nm corresponding to the dashed line in the topology image (c), XRD profile of the Cu_2S nanosheets showing α-chalcocite (d, RRUF ID: R120113.9).

To further elucidate the growth mechanism of nanodisks and the effects of supramolecular templating, we monitored nanodisk growth by stopping the thermolysis reaction of $CuSC_{12}H_{25}$ at various time intervals and analyzing the products by TEM (Figure 4). After 5 min of thermolysis, $CuSC_{12}H_{25}$ has only undergone a minor degree of decomposition. We observe small particles in aligned columns (Figure 4a). Based on XRD measurements and imaging contrast, most of the product observed by TEM corresponds to undecomposed $CuSC_{12}H_{25}$. After thermolysis has proceeded for 15 min, we observe the appearance of disk-like nanostructures. The nanodisks appear highly oriented within the dense organic matrix, suggesting that they precipitate within the aligned columns. After 30 min of thermolysis, we obtain the final nanodisk product. The nanodisks form aligned columns that appear to be embedded in a low density matrix, which we believe is undecomposed $CuSC_{12}H_{25}$. We have observed tracts of these aligned nanodisks over 1 μm long (corresponding to several thousand nanodisks). At thermolysis times longer than 30 min, the $CuSC_{12}H_{25}$ precursor is almost completely decomposed. We observe that the final nanodisks are free-standing (Figure 2b).

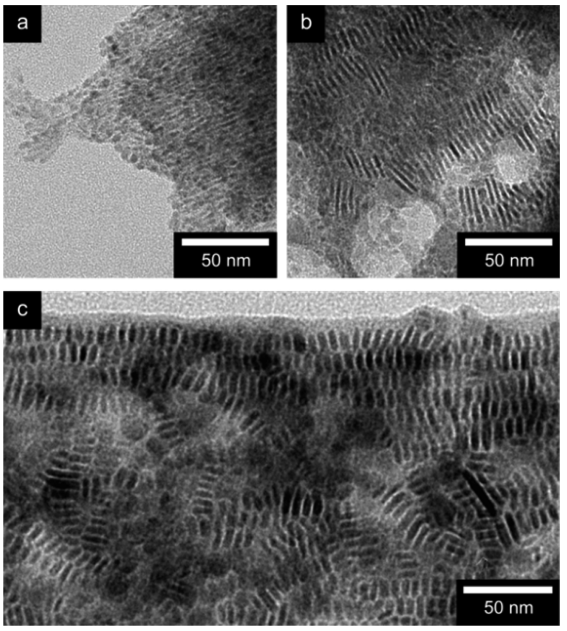

Figure 4. Time-dependent analysis. TEM images of $CuSC_{12}H_{25}$ precursor decomposed for various times: 5 min (a), 15 min (b), and 30 min (c).

These observations indicate that the discotic micelles serve as nucleation points for Cu_2S particles, which are templated into disks within the mesophase columns. Gradual thermal decomposition of the discotic micelles facilitates the transport of Cu alkanethiolate units to the outer surfaces of the stacked particles, enhancing radial growth. This is consistent with other reports where columnar mesophases have been shown to template nanowires[22] and nanoplates.[23]

To further demonstrate this mechanism of liquid crystalline templating, we carried out thermolysis reactions for non-mesogenic Cu thiolates. We chose ligands with steric groups that would preclude the formation of either the ordered lamellar or micellar phases. *tert*-Dodecanethiol ($CuSC(CH_3)_2C_9H_{19}$) possesses side-methyl groups that provide a large steric hindrance to close-packing; consequently, $CuSC(CH_3)_2C_9H_{19}$ is an isotropic liquid. Benzylmercaptan ($CuSCH_2Ph$) contains aromatic phenyl groups that produce radically different packing structures than alkanes due to π-stacking interactions. While $CuSCH_2Ph$ was isolated as a crystalline powder, the XRD spectrum revealed no evidence of lamellar order in the solid.

We carried out solventless thermolysis with both of these Cu thiolates at 200 °C for various reaction times. For $CuSC(CH_3)_2C_9H_{19}$, we also explored a range of thermolysis temperatures from 140 to 200 °C. Both Cu thiolates routinely yielded nano- and microparticles that were not uniform in size

dx.doi.org/10.1021/ja500786p | J. Am. Chem. Soc. 2014, 136, 6175−6178

or shape. These products were characterized by scanning electron microscopy (SEM) and XRD (Figure 5). Interestingly,

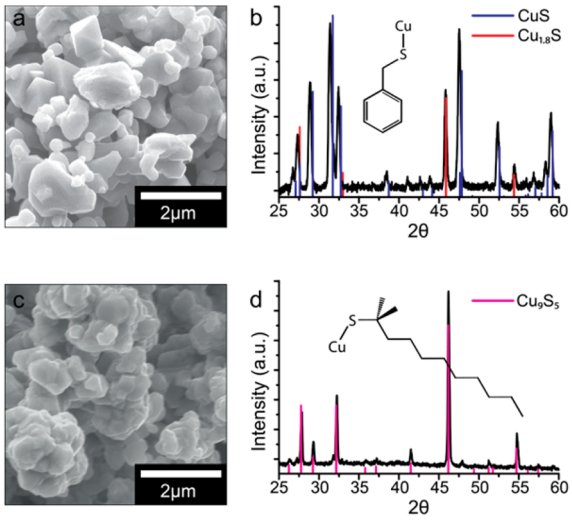

Figure 5. Decomposition of Nonmesogenic Cu Thiolates. SEM image (a) and XRD pattern (b) for the particles obtained from the thermolysis of $CuSCH_2Ph$ for 60 min at 200 °C, and SEM image (c) and XRD pattern (d) for the particles obtained from the thermolysis of $CuSC(CH_3)_2C_9H_{19}$ for 45 min at 200 °C.

the thermolysis products obtained from these thiolates are not composed of chalcocite, as with the nanodisk and nanosheet products. Instead, thermolysis of the nonlamellar Cu thiolates produced particles composed of digenite (Cu_9S_5) and covellite (CuS) phases, with traces of an intermediate $Cu_{1.8}S$ phase observed for decomposed $CuSCH_2Ph$. The higher sulfur content of these phases may be explained by the ability of both ligands to stabilize a carbocation on the primary carbon more favorably than a linear alkane. This would promote C−S bond cleavage over Cu−S bond cleavage, resulting in a higher retention of sulfur in the final solid-state product.

In conclusion, we show that supramolecular Cu alkanethiolates with varying chain lengths are able to template the formation of Cu_2S nanodisks and Cu_2S nanosheets. Melting of lamellar Cu alkanethiolates to the columnar mesophase is essential for generating the nanodisk shape. Nonmesogenic Cu thiolates produce irregularly shaped copper sulfide particles. Thus, supramolecular order of the Cu thiolate precursor dictates the resulting morphology of the nanocrystals obtained by thermolysis. This synthetic route has the potential to generate nanocrystal morphologies with highly anisotropic dimensions. These ultrathin semiconducting nanostructures may serve as key building blocks for nanoelectronic and optoelectric devices.

■ ASSOCIATED CONTENT

Ⓢ Supporting Information

Detailed synthetic procedure and Figures S1−S5. This material is available free of charge via the Internet at http://pubs.acs.org.

■ AUTHOR INFORMATION

Corresponding Author

atao@ucsd.edu

Notes

The authors declare no competing financial interest.

■ ACKNOWLEDGMENTS

This work was supported through a grant from the Office of Naval Research (Award No. N000141210574), and a grant from the National Science Foundation (CMMI, Award No. 1200850).

■ REFERENCES

(1) Wu, Y.; Wadia, C.; Ma, W.; Sadtler, B.; Alivisatos, A. P. *Nano Lett.* **2008**, *8*, 2551.
(2) Lee, H.; Yoon, S. W.; Kim, E. J.; Park, J. *Nano Lett.* **2007**, *7*, 778.
(3) Lai, C.-H.; Huang, K.-W.; Cheng, J.-H.; Lee, C.-Y.; Hwang, B.-J.; Chen, L.-J. *J. Mater. Chem.* **2010**, *20*, 6638.
(4) Luther, J. M.; Jain, P. K.; Ewers, T.; Alivisatos, A. P. *Nat. Mater.* **2011**, *10*, 361.
(5) Zhao, Y.; Pan, H.; Lou, Y.; Qiu, X.; Zhu, J.; Burda, C. *J. Am. Chem. Soc.* **2009**, *131*, 4253.
(6) Xie, Y.; Carbone, L.; Nobile, C.; Grillo, V.; D'Agostino, S.; Della Sala, F.; Giannini, C.; Altamura, D.; Oelsner, C.; Kryschi, C.; Cozzoli, P. D. *ACS Nano* **2013**, *7*, 7352.
(7) Hsu, S.-W.; On, K.; Tao, A. R. *J. Am. Chem. Soc.* **2011**, *133*, 19072.
(8) Mayer, K. M.; Hafner, J. H. *Chem. Rev.* **2011**, *111*, 3828.
(9) Angulo, A. M.; Noguez, C.; Schatz, G. C. *J. Phys. Chem. Lett.* **2011**, *2*, 1978.
(10) Tang, J.; Huo, Z.; Brittman, S.; Gao, H.; Yang, P. *Nat. Nanotechnol.* **2011**, *6*, 568.
(11) Kruszynska, M.; Borchert, H.; Bachmatiuk, A.; Rümmeli, M. H.; Büchner, B.; Parisi, J.; Kolny-Olesiak, J. *ACS Nano* **2012**, *6*, 5889.
(12) Ghahremaninezhad, A.; Asselin, E.; Dixon, D. G. *Electrochem. Commun.* **2011**, *13*, 12.
(13) Sigman, M. B.; Ghezelbash, A.; Hanrath, T.; Saunders, A. E.; Lee, F.; Korgel, B. A. *J. Am. Chem. Soc.* **2003**, *125*, 16050.
(14) Chen, Y. B.; Chen, L.; Wu, L. M. *Chem.—Eur. J.* **2008**, *14*, 11069.
(15) Wang, Y.; Hu, Y.; Zhang, Q.; Ge, J.; Lu, Z.; Hou, Y.; Yin, Y. *Inorg. Chem.* **2010**, *49*, 6601.
(16) Pablo Espinet, M. C. L.; Jose, M.; Martin-Alvarez. *Chem.—Eur. J.* **1999**, *5*, 1982.
(17) Levchenko, A. A.; Yee, C. K.; Parikh, A. N.; Navrotsky, A. *Chem. Mater.* **2005**, *17*, 5428.
(18) Sandhyarani, N.; Pradeep, T. *J. Mater. Chem.* **2001**, *11*, 1294.
(19) Baena, M. J.; Espinet, P.; Lequerica, M. C.; Levelut, A. M. *J. Am. Chem. Soc.* **1992**, *114*, 4182.
(20) Hsu, S.-W.; Bryks, W.; Tao, A. R. *Chem. Mater.* **2012**, *24*, 3765.
(21) Jennings, G. K.; Munro, J. C.; Yong, T.-H.; Laibinis, P. E. *Langmuir* **1998**, *14*, 6130.
(22) Siril, P. F.; Lehoux, A.; Ramos, L.; Beaunier, P.; Remita, H. *New J. Chem.* **2012**, *36*, 2135.
(23) Wang, L.; Chen, X.; Zhan, J.; Chai, Y.; Yang, C.; Xu, L.; Zhuang, W.; Jing, B. *J. Phys. Chem. B* **2005**, *109*, 3189.